

The First Absolute Central Moment In Low Level Image Processing

(A Plausible Mathematical Model of the First Stages of Biological Vision?)

Overview

The first absolute central moment belongs to the wide class of moments of n order, which includes variance, skewness and kurtosis. However, the first absolute central moment has not been analyzed in depth in the past and, in particular, its properties have never been exploited in image processing. It is common opinion that the first absolute central moment has not been investigated because of the mathematical difficulties introduced by the presence of the absolute value which makes theorem proving difficult.

Due to the absolute value involved, the first absolute central moment can be separated into two components: a positive deviation e_p and a negative deviation e_n . Once e_p and e_n are computed they can be combined. Derivative filters of both the first order and the second order can be obtained as well as mechanisms which are able to compensate the noise effects. Edges can be located and image key points such as corners, lines, line-endings and intersections between different discontinuities can be highlighted. The architectures of e_p and e_n and their responses to luminous stimuli recall the separation of the ganglion cells of a biological vision system into on-center off-surround and off-center on-surround cells.

The two positive and negative deviations e_p and e_n are themselves two mathematical operators which reveal interesting properties. e_p and e_n also highlight edges and lines with a ridge and provide local maxima at the image key points. While e_n provides a ridge with the peak at the dark border of a gray-level discontinuity, e_p provides a ridge with the peak at the bright border.

Other properties emerge from the analysis of the mass center of the first absolute central moment (vector \mathbf{b}). If vector \mathbf{b} is computed at a starting point p near an edge then vector \mathbf{b} joins a point p' which is closer to the edge than p , independently of the distance between p and the edge. Therefore, an iterative localization procedure can be developed by exploiting this property.

Due to the absolute value involved, vector \mathbf{b} also can be separated into two components: a positive component \mathbf{b}_p and a negative component \mathbf{b}_n . Once \mathbf{b}_p and \mathbf{b}_n are computed they can be combined: the sum $\mathbf{b}_p + \mathbf{b}_n$ is the mass center of the first absolute central moment (that is, vector \mathbf{b}) while the difference $\mathbf{b}_p - \mathbf{b}_n$ represents the normalized gradient of the gray-level image map.

The First Absolute Central Moment

Let $f(n,m)$ be the gray-level map of an image and let Θ_1 and Θ_2 be two concentric circular neighborhoods of a point \mathbf{p} with coordinates (n,m) . Let r_1 and r_2 , where $r_1 < r_2$, be the radii of Θ_1 and Θ_2 , respectively. The first absolute central moment can be computed as follows:

$$e(n,m) = \sum \sum_{\Theta_2} |\mu(n,m) - f(n-k, m-l)| g_2(k,l) \quad (1)$$

where the mean value $\mu(n,m)$ is computed as

$$\mu(n,m) = \sum \sum_{\Theta_1} f(n-k, m-l) g_1(k,l) \quad (2)$$

and $g_1(k,l)$ and $g_2(k,l)$ are two Gaussian weight functions with apertures σ_1 and σ_2 .

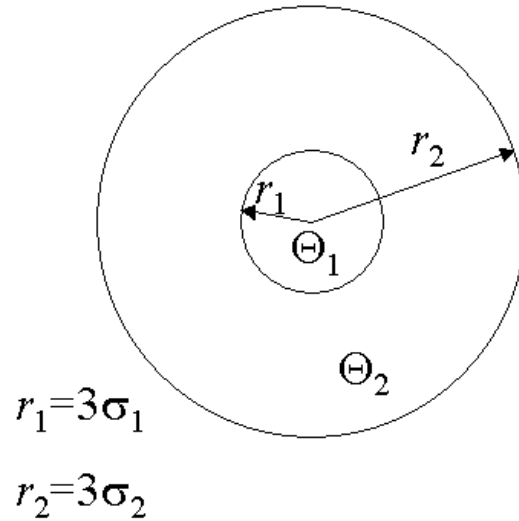


Fig.1

Even if simpler weight functions like box functions could be used, we prefer Gaussian functions since Gaussian has many qualities which make this function a unique operator in early image processing. In order to normalize the operator, the discrete Gaussian functions $g_1(k,l)$ and $g_2(k,l)$ are normalized over the circular neighborhoods Θ_i with radius $r_i = 3\sigma_i$. Eq.(1) measures the variability of the gray levels of the pixels which belong to the circular neighborhood Θ_2 of the image with respect to the local mean computed on the smaller circular neighborhood Θ_1 .

The Positive and Negative Deviations

The first absolute central moment $e(n,m)$ can be divided into two complementary filters: a positive deviation $e_p(n,m)$ and a negative deviation $e_n(n,m)$.

$$e_p(n,m) = \sum \sum_{\Theta_{2p}} (\mu(n,m) - f(n-k, m-l)) g_2(k,l) \quad (3)$$

$$e_n(n,m) = \sum \sum_{\Theta_{2n}} (\mu(n,m) - f(n-k, m-l)) g_2(k,l)$$

where the domains Θ_{2p} and Θ_{2n} are defined as

$$\Theta_{2p} = \{(k,l) \in \Theta_2 : \mu(n,m) > f(n-k, m-l)\} \quad (4)$$

$$\Theta_{2n} = \{(k,l) \in \Theta_2 : \mu(n,m) < f(n-k, m-l)\}$$

so that the first absolute central moment can be obtained as $e(n,m) = e_p(n,m) - e_n(n,m)$. Given the local mean $\mu(n,m)$ computed on the smaller circular neighborhood Θ_1 eqs.(3) measure the variability of the gray levels of the pixels, which belong to the circular neighborhood Θ_2 and which are greater or less than $\mu(n,m)$, respectively, with respect to $\mu(n,m)$ itself.

Fig.2 panel a) shows the response of both $e_p(n,m)$ and $e_n(n,m)$ given a test image with an ideal straight step discontinuity. At gray-level discontinuities $e_p(n,m)$ and $e_n(n,m)$ provide two ridges which overlap partially. The overlapping area is a thin ridge with a base equal to $2r_1$ where r_1 is the radius of Θ_1 . While $e_n(n,m)$ provides a ridge with the peak at the dark border of the gray-level discontinuity, $e_p(n,m)$ provides a ridge with the peak at the bright border. The figure shows also how the outputs of $e_p(n,m)$ and $e_n(n,m)$ can be combined to obtain different results at gray-level discontinuities.

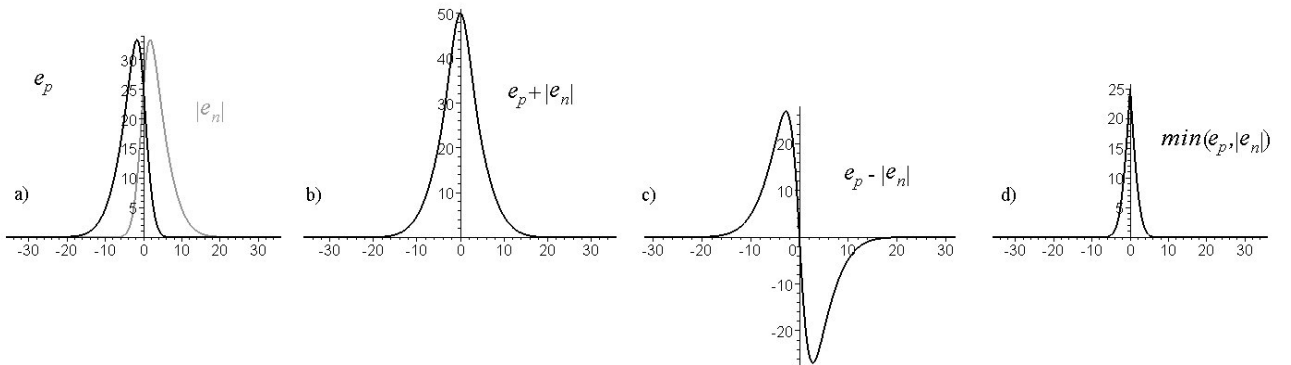


Fig.2

The negative deviation highlights dark structures on bright backgrounds and vice versa, the positive deviation highlights bright structures on dark backgrounds. According to this property, $e_p(n,m)$ and $e_n(n,m)$ can be used to highlight the outer and inner border of structures in interest separately.

A Filter Analogous to the GoG Filter

When we subtract the output of $e_n(n,m)$ from $e_p(n,m)$ the output of the first absolute central moment $e(n,m)$ is obtained. While $e(n,m)$ is equal to zero over homogeneous regions, at discontinuities $e(n,m)$ provides a ridge and the ridge peaks locate the points of the discontinuity. The first absolute central moment is a dispersion index which provides a ridge map similar to the ridge map provided by the magnitude of a standard GoG (gradient of Gaussian) operator.

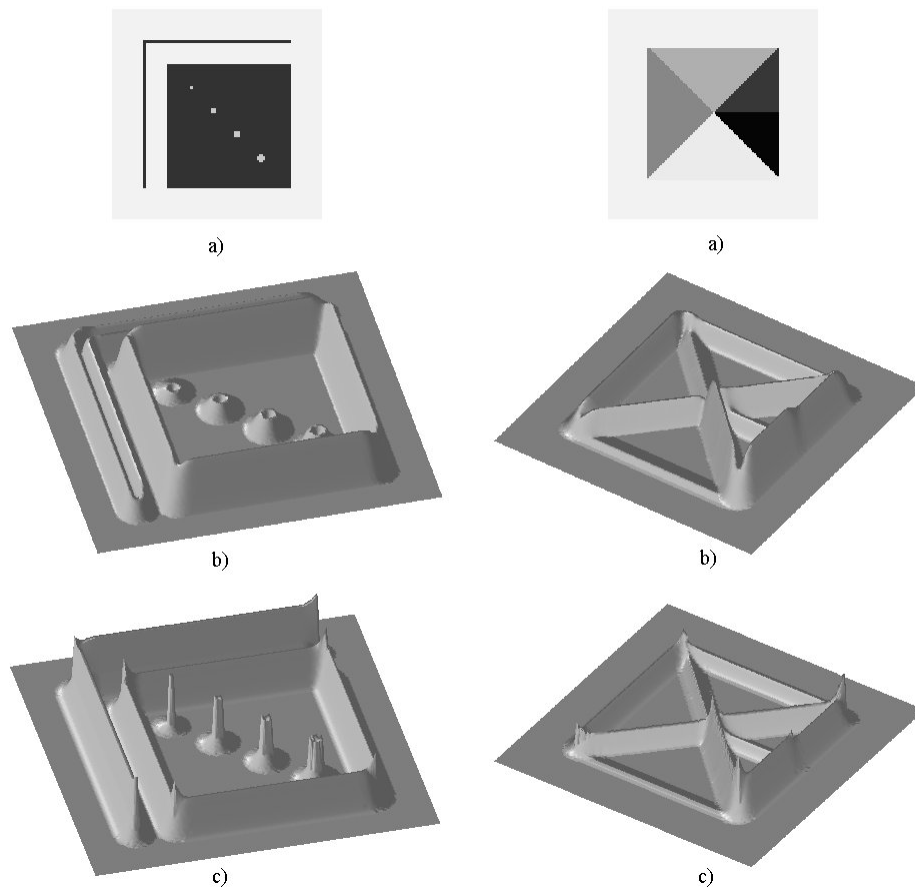


Fig.3

Fig.2 panel b) shows how the linear combination $e_p(n,m) - e_n(n,m)$ provides a ridge at discontinuities. However, unlike the magnitude of the GoG, the first absolute central moment provides ridges at edges and lines and gives rise to local extrema of the ridges at key points such as line endings, corners, spots and junctions. Fig.3 shows two test images in panels a) and the relative ridge maps provided both by the first absolute central moment (panels c)) and by an equivalent GoG filter (panels b)). However, it is worth noting that the first absolute central moment cannot highlight particular junctions with a local maximum. Local maxima at all the junctions can be ensured only if the two positive and negative components (e_p and e_n) of the first absolute central moment are kept separated.

The same Output of a Standard DoG Filter

The first central moment can be obtained by adding the negative deviation to the positive deviation. It is worth noting, however, that in our case the radius of Θ_1 is smaller than the radius of Θ_2 and the obtained operator $c(n,m)$ is a generalized first central moment rather than a real first central moment.

$$c(n,m) = \sum \sum_{\Theta_2} (\mu(n,m) - f(n-k, m-l)) g_2(k,l) \quad (5)$$

Since $c(n,m)$ is obtained by eliminating the absolute value brackets in eq.(1), then by developing eq.(5) we obtain:

$$\begin{aligned} c(n,m) &= e_p(n,m) + e_n(n,m) = \\ &= f(n,m) \otimes (g_1(n,m) - g_2(n,m)) \end{aligned} \quad (6)$$

where \otimes is the convolution operator. Eq.(6) shows how adding $e_p(n,m)$ to $e_n(n,m)$ is equivalent to filtering the image $f(n,m)$ with a standard DoG filter. Fig.2 panel c) shows how the linear combination $e_p(n,m) + e_n(n,m)$ provides a zero-crossing at discontinuities.

A Simple Zero-Crossing Map

We have seen how adding $e_p(n,m)$ to $e_n(n,m)$ is equivalent to filtering the image $f(n,m)$ with a standard DoG filter independently of the apertures σ_1 and σ_2 . However, where the two positive and negative DoG components cross the zero (that is, at the zero-crossing points), the two ridges provided by the positive and negative central deviations overlap partially. The profile of the overlapping area is that of a thin ridge and the peak of the ridge locates the discontinuity; the greater the discontinuity, the higher the peak. Consequently, the function $\text{Min}(\text{positive deviation}, |\text{negative deviation}|)$ provides both the zero-crossing map and an estimate of the image luminance variation (the zero-crossing strength). Fig.2 panel d) shows how the function M_{pn} provides a thin ridge at a step discontinuity. Fig.3.1 shows how the function M_{pn} provides a thin ridge at the gray level discontinuities of the test images of Fig.4.

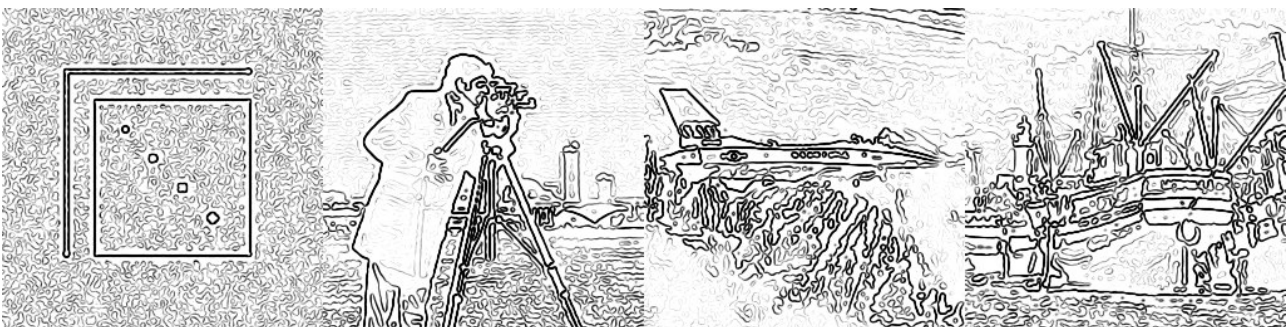


Fig.3.1

A Local Thresholding Procedure

A local thresholding procedure can be achieved by combining two ridge maps obtained when two different sets of low-pass filters are used. The difference in noise compensation given by the two following filtering processes has been analyzed:

$$e_1(n,m) = \sum \sum_{\Theta_2} |\mu(n,m) - f(n-k,m-l)| g_2(k,l) \quad (7)$$

$$\mu(n,m) = \sum \sum_{\Theta_1} f(n-k,m-l) g_1(k,l)$$

$$e_2(n,m) = g_3(n,m) \otimes \sum \sum_{\Theta_2} |f(n,m) - f(n-k,m-l)| g_2(k,l) \quad (8)$$

Provided that $\sigma_1 = \sigma_3$, eq.(7) provides a lower noise level than eq.(8). The opposite result, however, is obtained at the discontinuities. While in eq.(8) the height of the ridges at the discontinuities obviously decreases by filtering the central deviation $e(n,m)$ with the Gaussian $g_3(n,m)$, in eq.(7) the height of the ridges at the discontinuities does not decrease when the Gaussian $g_1(n,m)$ is used.



Fig.4

Therefore, as eq.(7) produces both higher ridges and a lower noise level than eq.(8), the map obtained by the filtering process (8) can be used as a threshold map of the ridge map obtained by the filtering process (7). Fig.4 shows the test images and the result of the thresholding process. In particular, the first panel shows the robustness of the thresholding process to additive Gaussian noise.

The Mass Center of the Gray Level Variability

The first absolute central moment is a statistical filter which measures the variability of the gray levels of the image with respect to the local mean. The function $h(\mathbf{p}, k, l)$

$$h(\mathbf{p}, k, l) = |\mu(\mathbf{p}) - f(n-k, m-l)| g_2(k, l) \quad (9)$$

which can be found in eq.(1) describes the spatial distribution of the variability of the gray levels with respect to the local mean computed at point $\mathbf{p}=(n, m)$. The function $h(\mathbf{p}, k, l)$ can be seen as a mass function which associates a mass value to every pixel surrounding \mathbf{p} and the first absolute central moment $e(\mathbf{p})$ can be seen as the total mass of the variability of the gray levels at point \mathbf{p} . Therefore, the center of mass of the gray-level variability at point \mathbf{p} is computed with the vector $\mathbf{b}(\mathbf{p})$:

$$\mathbf{b}(\mathbf{p}) = \begin{cases} \frac{1}{e(\mathbf{p})} \sum \sum_{\Theta_2} h(\mathbf{p}, k, l) \mathbf{\Gamma} & \text{if } e(\mathbf{p}) \neq 0 \\ 0 & \text{if } e(\mathbf{p}) = 0 \end{cases} \quad (10)$$

where $\mathbf{\Gamma}$ is a vector which has $-k, -l$ components.

Let us consider a gray-level discontinuity and a point \mathbf{p}_0 close to the discontinuity. Vector \mathbf{b} always indicates the discontinuity. Moreover, when particular configurations of eq.(10) are chosen, vector \mathbf{b} locates a point \mathbf{p}_1 which is closer to the discontinuity than \mathbf{p}_0 independently of the distance between \mathbf{p}_0 and the discontinuity. Hence, given a starting point the closest point of a discontinuity can be located by iteratively computing vector \mathbf{b} .

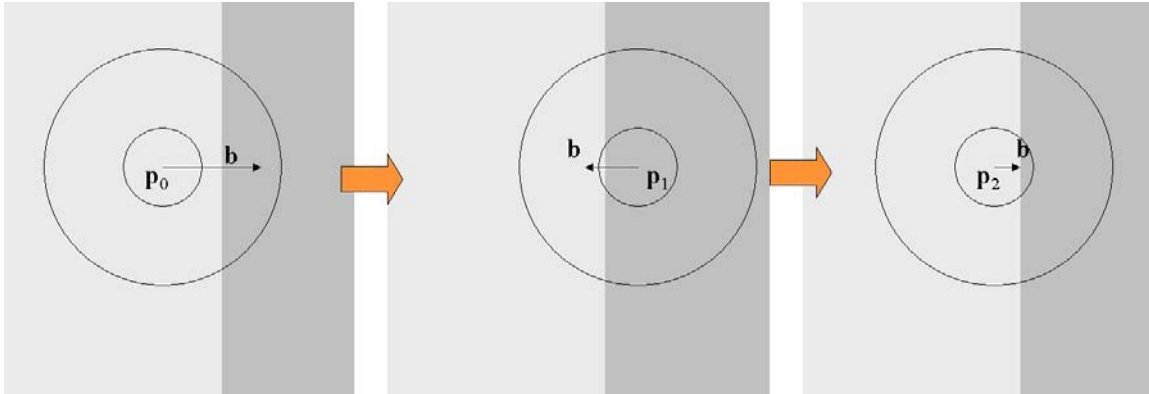


Fig.5

An Edge Localization Procedure

Let $|\varepsilon|$ be the distance of \mathbf{p} from a straight discontinuity, vector $\mathbf{b}(\mathbf{p})$ was computed and the following relationship was obtained

$$b(\varepsilon) = -\frac{\sigma_2 \sqrt{2} e^{-\frac{\varepsilon^2}{2\sigma_2^2}}}{\sqrt{\pi}} \frac{\operatorname{erf}\left(\frac{\varepsilon\sqrt{2}}{2\sigma_1}\right)}{1 - \operatorname{erf}\left(\frac{\varepsilon\sqrt{2}}{2\sigma_1}\right)\operatorname{erf}\left(\frac{\varepsilon\sqrt{2}}{2\sigma_2}\right)} \quad (11)$$

Vector \mathbf{b} always indicates the discontinuity and its magnitude is symmetric with respect to the discontinuity. Fig.6 shows how the magnitude of the vector $\mathbf{b}(\varepsilon)$ varies for positive values of ε when $\sigma_2 = 4\pi$ pixels. The mass center computed at \mathbf{p} approaches the discontinuity independently of the distance between \mathbf{p} and the discontinuity if $|\mathbf{b}(\varepsilon)| < 2|\varepsilon|$ for every value of ε . From eq.(11) it is easy to show that the magnitude of vector \mathbf{b} decreases when σ_1 increases, independently of the values of ε and σ_2 , and that the condition $\sigma_1 > \sigma_2/\pi$ is a necessary condition to satisfy the inequality $|\mathbf{b}(\varepsilon)| < 2\varepsilon$ for every positive value of ε . Therefore, when the first absolute central moment is used, the mass center of the gray-level variability always approaches the discontinuity if the relationship $\sigma_1 > \sigma_2/\pi$ is satisfied. We are currently using such a procedure to track contours automatically and in real time through sequences of echographic images.

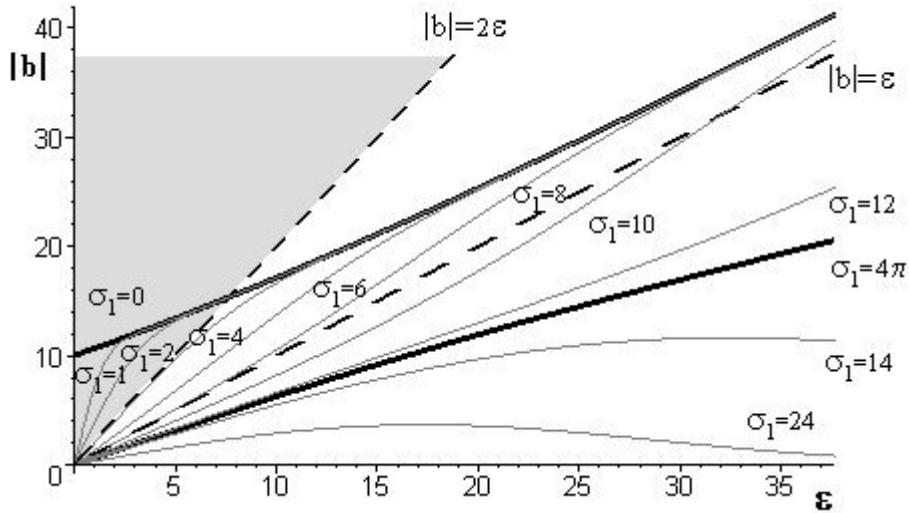


Fig.6

An Operator Analogous to a Normalized Gradient

Here again the two positive and negative components of vector \mathbf{b} can be introduced

$$\begin{aligned} \mathbf{b}_p(\mathbf{p}) &= \frac{1}{e(\mathbf{p})} \sum \sum_{\Theta_{2p}} h(\mathbf{p}, k, l) \Gamma & \text{if } e(\mathbf{p}) \neq 0, & \quad \mathbf{b}_p(\mathbf{p}) = 0 & \text{if } e(\mathbf{p}) = 0 \\ \mathbf{b}_n(\mathbf{p}) &= \frac{1}{e(\mathbf{p})} \sum \sum_{\Theta_{2n}} h(\mathbf{p}, k, l) \Gamma & \text{if } e(\mathbf{p}) \neq 0, & \quad \mathbf{b}_n(\mathbf{p}) = 0 & \text{if } e(\mathbf{p}) = 0 \end{aligned} \quad (12)$$

where the domains Θ_{2p} and Θ_{2n} are defined in eqs.(4). Vector \mathbf{b} is obviously obtained by adding the negative component \mathbf{b}_n to the positive component \mathbf{b}_p ($\mathbf{b}(\mathbf{p}) = \mathbf{b}_p(\mathbf{p}) + \mathbf{b}_n(\mathbf{p})$). However, a different operator \mathbf{b}_g is obtained by subtracting \mathbf{b}_n from \mathbf{b}_p : that is, by eliminating the absolute value brackets in eq.(9).

$$\mathbf{b}_g(\mathbf{p}) = \begin{cases} -\frac{1}{e(\mathbf{p})} \sum \sum_{\Theta_2} f(n-k, m-l) \Gamma g_2(k, l) & \text{if } e(\mathbf{p}) \neq 0 \\ 0 & \text{if } e(\mathbf{p}) = 0 \end{cases} \quad (13)$$

The summation in eq.(13) represents the convolution of the function $f(n, m)$ with the gradient of the Gaussian function $g_2(n, m)$ since, except for a constant factor, the term $\Gamma g_2(k, l)$ is exactly the gradient of the function $g_2(k, l)$. On the other hand, as we have seen, the normalizing factor $e(\mathbf{p})$ is very similar to the magnitude of the gradient of Gaussian. Therefore, given a gray-level image map $f(n, m)$, vector \mathbf{b}_g provides the same information of a normalized gradient of Gaussian. A normalized gradient is needed, for example, to derive the velocity vector from the optical-flow equation.

Summary

The most interesting feature of the first absolute central moment is that the generalization of this simple dispersion index gives rise to a class of filters, the outputs of which can be in turn usefully combined.

The first central moment, which is obtained by adding the negative deviation to the positive deviation, provides a map which is equal to the one provided by a standard DoG filter. The simple algebraic function $\text{Min}(\text{positive deviation}, |\text{negative deviation}|)$ can also provide both the zero-crossing map and an estimate of the image luminance variation. Moreover, a simple thresholding procedure can be obtained by combining two maps provided by two different filtering processes. The first absolute central moment, which is obtained by subtracting the negative deviation from the positive deviation, provides a ridge map which is similar to the one provided by the GoG filter. However, unlike the GoG, the absolute moment provides ridges at edges and lines and gives rise to local extrema of the ridges at line endings, corners and junctions.

In addition, given a starting point, the closest point of a discontinuity can be located with just a couple of jumps by iteratively computing the mass center of the first absolute central moment (vector \mathbf{b}). We are currently using such an operator to track contours in real time through sequences of echographic images. Finally, an operator very similar to a normalized gradient of the gray-level image map is obtained when subtracting the negative component of vector \mathbf{b} from its positive component.

To conclude, we wish to point out that all the possible combinations of the edge information, recovered by the class of filters generated by the generalization of the first absolute central moment, have not been analyzed. Since three different low-pass filters can be introduced into two nonlinear filters (positive and negative deviations) a large class of filters is obtained and possible combinations of the recovered edge information still remain to be investigated. The edge detection properties of the two negative and positive deviations when used separately also remain to be investigated in depth. These two operators should be analyzed separately and their analysis should be compared with the knowledge achieved on the low level stages of the biological vision systems since their architectures and their responses to luminous stimuli recall the separation of the ganglion cells into on-center off-surround and off-center on-surround cells.